CDK12/13 Inhibition Induces Immunogenic Cell Death and Enhances Anti-PD-1 Anticancer Activity in Breast Cancer

Yi Li
Sichuan Academy of Medical Sciences and Sichuan People's Hospital
Hui Zhang
Sichuan Academy of Medical Sciences and Sichuan People's Hospital
Qin Li
University of Electronic Science and Technology of China
Pingjin Zou
University of Electronic Science and Technology of China
Xingxiang Huang
University of electronic science and technology of China
Chihua Wu
Sichuan Academy of Medical Sciences and Sichuan People's Hospital
Li Tan (tanlics@med.uestc.edu.cn)
Sichuan Academy of Medical Sciences and Sichuan People's Hospital

Research

Keywords: SR-4835, PD-1, immunotherapy, immunogenic cell death, CDK12/13

Posted Date: August 20th, 2020

DOI: https://doi.org/10.21203/rs.3.rs-60828/v1

Version of Record: A version of this preprint was published at Cancer Letters on December 1st, 2020. See the published version at https://doi.org/10.1016/j.canlet.2020.09.011.

Abstract

Background: The T cell response against different tumors is improved by immunogenic cell death (ICD), indicating a role for ICD in augmenting antitumor immunity elicited by the anti-checkpoint antibody anti-programmed death 1 (anti-PD-1).

Methods: The effect of SR-4835 on breast cancer was analyzed by cell proliferation and flow cytometry. Calreticulin translocation and HMGB1 and ATP release were detected by flow cytometry, ELISA and luminescence assay, respectively. Immunogenicity in vitro was analyzed by co-culturing of SR-4835 treated cancer cells with bone-marrow derived dendritic cells (BMDCs) and rate of maturation of BMDCs and production of IL-6 in the supernatant were measured. The in vivo antitumor effect was analyzed by syngeneic mouse model followed by flow cytometry for TILs.

Results: In the present study, we report a synergistic and durable immune-mediated antitumor response elicited by the combined treatment of SR-4835, a CDK12/13 specific inhibitor, with PD-1 blockade in a murine model of 4T1 breast cancer. The developed combination therapy elicited antitumor activity in immunocompetent mouse tumor models. Furthermore, the SR-4835-treated tumor cells exhibited characteristics of ICD, including the release of high mobility group box 1 (HMGB1) and ATP and the translocation of surface calreticulin (CRT). This activity led to a significant T-cell dependent regression of tumors. The enhanced infiltration of T cells and dendritic cell (DC) activation in the tumors of mice treated with both SR-4835 and anti-PD-1 indicate that this combination treatment promotes an improved immune response and suggests a potential mechanism involving anti-PD-1 and SR-4835 activity that enhances anti-PD-1 effects.

Conclusion: The results of the present study demonstrate the potential of CDK12/13 inhibition combined with checkpoint inhibition in breast cancer treatment.

Introduction

In women, breast cancer represents nearly one-third of newly diagnosed cancers and is the most common cancer in women from ages 20 to 59(1). Currently, breast cancer treatments are based on the expression of biomarkers, such as progesterone receptor (PR), estrogen receptor (ER), and human epidermal growth factor receptor 2 (EGFR2, also known as HER2)(1, 2). Good clinical outcomes have been observed after anti-hormonal therapies in tumors expressing ER, although these therapies lead to resistance, limiting the effectiveness of hormone-based therapy (3). Triple-negative breast cancer (TNBC) is a subtype in which PR, ER and EGFR2 are not expressed (4–6). With no approved targeted therapy, TNBC is the most aggressive breast cancer, with the worst prognosis and the highest mortality rates (5). The primary treatment options for TNBC include radiation- and chemotherapies, and surgical resection, which have limited efficacy and are accompanied with severe side effects (4). Thus, it is imperative to identify novel drugs that can effectively treat and prevent breast cancer, particularly TNBC, with minimum side effects.

Over the past years, treatments that target and kill cancer cells by using or strengthening the immune system of patients have been developed (7, 8), with antibodies targeting inhibitory signaling molecules expressed on immune and tumor cells being commonly used treatment modalities (9, 10). Typical targets include cytotoxic T-lymphocyte associated protein 4 (CTLA4) and the immune checkpoint proteins programmed death-1 (PD-1), and PD-1 ligand (PD-L1) (11). Across various cancers, initial treatment using a monoclonal antibody against anti-PD-1 has been effective clinically, and these successes have driven the field of cancer immunotherapy (12). Upon activation, T lymphocytes express PD-1, and upon exhaustion, these T cells do not respond to stimulation (13). To prevent excessive inflammation, PD-1 delivers an inhibitory signal and acts as a regulatory molecule (14). Positive prognostic factors include the expression of an IFN-γ gene signature as well as neoantigens, PD-1 expression, the presence of tumor-infiltrating lymphocytes (TILs), and a high mutational load (15). Tumors lacking intrinsic antigen presentation or with no T cells that can respond to antigens are remarkably less likely to react to anti-PD-1 (15, 16). Thus, in tumors that are typically immunosuppressed or immunologically barren, therapies that create an immunogenic environment can potentially benefit a greater number of patients from anti-PD-1 treatment (16).

Tumor cells are antigenic, indicating that their genomes are significantly abundant in somatic mutations (17). However, these cells have a low propensity to elicit cytotoxic T cell responses because host immunity activation processes, such as presentation of antigen, function under immunosuppressive tumor conditions (18). Accordingly, the death of cancer cells can be immunogenic or non-immunogenic depending on the initiating stimulus (19). Some chemotherapeutics are known to induce the immunogenic cell death (ICD) of cancer cells, including oxaliplatin, mitoxantrone, and doxorubicin (Dox), thereby initiating antitumor immune response activation (20). The effect of ICD inducers has been shown to be adaptive immunity-independent in some spontaneous mammary tumor models, indicating the insufficiency of ICD inducers in the induction of effective antitumor immunity (21). Therefore, we hypothesized that the effective ‘awakening’ of intrinsic tumor immunity may occur through a suitable combined antitumor immunotherapy using an ICD inducer along with a phagocytosis enhancer to promote the immunogenic killing of tumor cells.

The cyclin-dependent kinase CDK12 forms a heterodimeric complex with cyclin K, its activating partner, and modulates various important functions in cells (22). CDK12 harbors different functional domains, including several arginine/serine (RS) motifs at the N-terminus, a central kinase domain, and a proline-rich motif (PRM) that can act as a binding site for additional proteins (23). The direct regulation of transcription by CDK12 involves the phosphorylation of serine residues within heptapeptide repeats (YSPTSPS) at the RNA polymerase II C-terminal domain necessary for transcriptional elongation (24). Previous study has shown that CDK4/6 inhibitors sensitizes antitumor effect of anti-PD-1 antibody via regulating PD-L1 stability (25), or enhancing T cell activation (26). Furthermore, dinaciclib, a CDK2 inhibitor, was found enhances anti-PD1-mediated tumor suppression by inducing immunogenic cell death(27). Thus, we hypothesis if CDK12/13 inhibitor promotes the antitumor effect of anti-PD1 antibody and investigated the underlying mechanisms.

In the present study, we show that CDK12/13 inhibitor-mediated enhancement of tumor immunogenicity can improve overall anti-PD-1 checkpoint blockade efficacy in breast cancer.

Materials And Methods

Cell lines

The human breast cancer cell lines MCF-7, T47D, MDA-MB-231 and MDA-MB-468 and mouse 4T1 cells were obtained from the American Type Culture Collection (ATCC) and were authenticated to be free of mycoplasma. Cells were cultured in RPMI 1640 medium (Gibco) containing fetal bovine serum (FBS, 10%; Corning) and 1% penicillin and streptomycin (10,000 U/mL; Life Technologies) at 37 ℃ in a humidified incubator and under a 5% CO_2 atmosphere. DMSO (Sigma) was used to dissolve SR-4835.

The Cell Proliferation Assay

CellTiter 96 AQueous One Solution from Promega was used to assess cell viability. Cells were seeded at 5×10^3 cells/well in 96-well plates (Corning) and allowed to adhere overnight. Then, after 48 hours, the absorbance at 490 nm was measured on a microplate reader.

Determination of surface CRT, apoptosis, ATP and HMGB1 release

4T1 cells were grown to 40-50 % confluence in 6-well plates, washed, and then incubated with increasing concentrations SR-4835 for one day. Tumor cell death induced by SR-4835 was assessed using an Apoptosis Detection Kit Annexin V/Propidium Iodide kit (eBioscience), and surface CRT was detected by flow cytometry. The supernatants of cells cultured under the same conditions described above were evaluated for extracellular HMGB1 levels using an ELISA kit (Chondrex). Extracellular ATP was quantified using an ENLITEN ATP Assay System Bioluminescence Detection Kit (Promega), and chemiluminescence derived from ATP was detected on a Multi-Mode Plate Reader Analyst HT (LJL BioSystems).

Western blotting

Western blotting was performed as described in previous studies (28, 29). Briefly, cell lysates were prepared by suspending harvested cells in cell lysis buffer (50 mM NaCl, 25 mM HEPES, 10% glycerol, 5 mM EDTA, and 1% Triton-X-100) containing protease and phosphatase inhibitors (Mini Protease Inhibitor cocktail from Roche; 1 μM PMSF, 50 mM sodium fluoride, 50 mM sodium pyrophosphate, and 1 μM sodium orthovanadate,). The protein concentration of the samples was measured using a BCA Protein Assay kit from Pierce. The samples were prepared under reducing conditions, loaded into pre-cast 10% gels and electrophoresed at 200 V. Then, the resolved proteins were transferred on to a PVDF membrane (Sigma), blocked at room temperature in bovine serum albumin (5%)/PBS-Tween 20 (0.001%) for 60 min, incubated at 4 ℃ overnight with a primary antibody prepared in BSA/PBS-T (5%) and then incubated with horseradish peroxidase-conjugated goat secondary antibody for 60 min. Detection of bound secondary antibody was performed using the Supersignal West Femto Maximum Sensitivity Substrate

detection system from Pierce, and the signals were analyzed using Image Lab software and a ChemiDoc Imager (both from Bio Rad).

Determination of glucose uptake

Cells were added to 96-wells and treated with SR-4835. Then, after 24 hours, glucose uptake was evaluated using a Glucose Uptake-Glo™ Assay (Promega) following the manufacturer's instructions.

Cytokine release, dendritic cell activation, and phagocytosis assays.

The femurs of BALB/c mice were used to harvest BM cells, which were cultured in complete RPMI supplemented with 50 ng/mL recombinant mouse GMCSF and 25 ng/mL of IL-4 (Peprotech) for one week to generate $CD11c^+$ DCs (dendritic cells). 4T1 tumor cells were labeled with DiO (Life Technologies) and treated for 24 hours with SR-4835 before being cultured with DCs at a 2:1 ratio for one day. Then, the cells were stained with fluorescently labeled antibodies against CD80, CD11c, CD86, CD83 and MHCII (BioLegend) and analyzed by flow cytometry. The detection of a CD11c (DC)/DiO (tumor)/double-positive signal was evaluated for tumor phagocytosis. IL-1β, TNF-α, IL-6 and IL-12p70 levels in coculture supernatants were detected using a V-PLEX Meso Scale Discovery Assay, and antigen presentation in tumors by DCs was assessed using anti-H-2Kb-SIINFEKL (BioLegend clone 25-D1.16).

Syngeneic tumor models.

The maintenance of mice and the experiments performed in the present study were approved by the Animal Use and Care Committee of Sichuan Academy of Medical Sciences & Sichuan Provincial People's Hospital, School of Medicine. BALB/c mice (female, 4-6 weeks old) were procured from Charles River Laboratory. 4T1 cells (5×10^5 cells) were subcutaneously injected into the right flanks of mice. When the tumor volume reached 50-100 mm^3 (day 0), mice were arbitrarily split into groups and treated with SR-4835, anti-mouse PD-1, and their combination. Treatments were administered every two days for 30 days. Every two days, tumor dimensions were measured using a caliper, and the volume was determined as per the formula: Volume (mm^3) $=L\times W^2/2$, where L and W indicate the length and width of the tumor (both in mm), respectively.

BALB/c mice (4-6 weeks old) were used to study CD8 depletion. Upon reaching 50-100 mm^3 in volume, the mice were placed into PBS, CD8 depletion, combination treatment, and CD8 depletion plus combination treatment groups. Mice in the CD8 depletion group were injected with 200 μg of antibodies to deplete CD8 (clone 53.6.7; BioXcell).

TIL isolation.

After two treatments, the mice were sacrificed and the tumors were excised. Then the, tumors were mechanically disrupted using a GentleMACS Dissociator (Miltenyi Biotec) along with enzymatic digestion using a Tumor Dissociation kit (Miltenyi Biotec). To stain cytokines within the cells, T cells in PBS were

analyzed via phosphoflow flow cytometry using a fixable live/dead stain after staining antibody surface markers of cells in FACS buffer (PBS with 0.1% sodium azide and 0.5% BSA). Then, the cell surface molecules were stained, after which the cells were fixed and permeabilized (eBioscience) for intracellular staining. To stain cytokines, cells were stimulated with Cell Stimulation Cocktail (eBioscience) with PMA/ionomycin and then treated with a protein transport inhibitor prior to staining. The cells were fixed in formaldehyde (4%) and then permeabilized with methanol (100%) for phosphostaining. Then, the cells were analyzed by flow cytometry (LSRII; BD Bioscience), with data analysis performed using FlowJo (TreeStar).

Statistical analysis

GraphPad Prism 7 (GraphPad Software) was used for data analyses. Two-tailed Student's *t*-test was used for statistical analyses. Bonferroni's post-test was used after one or two-way ANOVA between multiple treatment groups to assess the significance of the differences. The data are presented as the means ± SD (standard deviation). Differences were considered significant at $P < 0.05$.

Results

SR-4835 promotes ICD induction in breast cancer cells

4T1 cells treated with SR-4835 were assessed for cell death. The results showed a reduction in 4T1 cell viability (**Figure 1A**) and an increase in apoptosis (**Figure 1B**) upon SR-4835 treatment in a dose-dependent manner. Similar results were obtained in human breast cancer cells with differences in hormone epidermal growth factor receptor 2 (HER-2), estrogen receptors (ER), and progesterone receptor (PR) expression, including MCF-7, T47D, MDA-MB-231 and MDA-MB-468 cells (**Figure 1C and 1D**). Based on previous research, not every cell death modality is immunogenic and causes anti-tumor effects (19, 30, 31) , with *in vitro* ICD identification primarily depending on the detection of damage-associated molecular patterns (DAMPs) (32). Therefore, we assessed 4T1 cells with respect to the role of plasma on the viability of cells and the effects of DAMP signaling, including ATP secretion and CRT translocation.

The surface exposure of CRT regulates the immunogenicity of dying cancer cells (33) . Although present on the ER membrane, CRT sends an 'eat me' DAMP signal on the cell surface that triggers the APC-mediated identification, engulfment, and processing of tumor cells (34) . After one day of SR-4835 treatment, the presence of CRT on the surface was measured. Anti-CRT antibodies were used to label intact cells, which were then stained with secondary fluorescent antibodies and evaluated by flow cytometry. We observed a dose-dependent increase in CRT levels on the surfaces of 4T1, T47D and MDA-MB-231 cells, indicating that the immunogenicity of these cells increased due to the SR-4835 treatment (**Figure 1E-1F**). An important molecule for metabolism is ATP, which is secreted by cells during the process of ICD (35) . ATP secretion even involves pathways that intersect with CRT externalization (35). ATP is involved in ICD once it reaches the extracellular space and acts as a 'find me' DAMP signal to promote the engagement and activation of APCs (36) . To assess this DAMP secreted by SR-4835-exposed cells, the cell culture supernatant was collected 10 minutes post-treatment and assessed for

extracellular ATP levels, which were observed to increase (**Figure 1G and 1H**). Furthermore, the secretion of HMGB1 by SR-4835-treated 4T1 cells also increased (**Figure 1I and 1J**). Taken together, these results suggest that ICD is induced by SR-4835 in breast cancer cells.

SR-4835 induces endoplasmic reticulum (ER) stress through metabolic changes

The ER plays a major role in intracellular signaling pathways that induce ICD (37). The ER stress response begins after initiation eIF2α, a eukaryotic translation factor, becomes phosphorylated, and this protein has also been put forward as an ICD marker (38). Thus, we assessed the level of eIF2α phosphorylation in SR-4835-treated 4T1 cells and observed enhanced eIF2α phosphorylation at serine 51 (**Figure 2A**). In addition to eIF2α, inositol-requiring enzyme 1 (IRE1), another ER protein acting as a sensor of ER stress, mediates the unfolded protein response (UPR) (39) . Similar to the activation of eIF2α, an increase in the phosphorylation of IRE1 was observed in SR-4835-treated 4T1 cells (**Figure 2A**). In addition, we also observed p-PERK and BIP upregulation upon SR-4835 treatment (**Figure 2A**), and the upregulation of p-eIF2α, IRE1, p-PERK, and BIP levels was also observed in T47D and MDA-MB-231 cells after SR-4835 treatment (**Figure 2B and 2C**). Thus, our findings suggest SR-4835 initiates the ER stress response, which is associated with ICD in breast cancer cells.

ER processes rely on sources of extrinsic energy provided through glycolysis or oxidative phosphorylation (40) . Therefore, we explored if changes in glucose metabolism have a role in extracellular ATP increase. Glucose uptake is the first important step in glucose metabolism, and glucose uptake was observed to be significantly decreased in 4T1, T47D and MDA-MB-231 cells after SR-4835 treatment (**Figure 2D-2F**). This decrease may be due to the dysregulation of several metabolic steps, such as a decrease in glucose transport. Therefore, we subsequently evaluated the levels of glucose transporters, in these treated cells and observed a significant decrease in GLUT3 protein levels (**Figure 2G-2I**). Therefore, the induction of ER stress due to SR-4835 occurs possible via ATP secretion, which results from reduced glucose transporter levels, ultimately causing reduced glucose uptake.

SR-4835 enhances DCs function in 4T1 cells

Because DCs play an important role in recognizing ICD-associated DAMPs followed by tumor antigen uptake and presentation (41) , we examined the phagocytosis of SR-4835-treated tumor cells by DCs. We cultured SR-4835-treated 4T1 cells with mouse bone marrow-derived DCs (BMDCs) and observed efficient DC phagocytosis of the treated tumor cells (**Figure 3A**), which caused enhanced maturation of DCs, as shown by MHCII, CD86, CD80 and CD83 surface expression (**Figure 3B-3E**). Furthermore, the coculture supernatant exhibited increased IL-1β, TNF-α, IL-6 and IL-12p70 levels (**Figure 3F-3I**). Thus, our findings indicated that SR-4835 promotes DC activation in cancer cells.

Finally, the immunogenic potential of SR-4835 was assessed in a vaccine setting. Immunocompetent BALB/c mice were injected with 4T1 tumor cells treated with SR-4835 *in vitro*. Ten days later, the mice were challenged again by injecting live tumor cells, and the mice immunized with SR-4835-treated dead tumor cells exhibited enhanced tumor-free survival compared with those injected with tumor cells that

were freeze-thawed (**Figure 3J**). Taken together, these results suggest that SR-4835 promotes ICD induction in this model.

αPD-1 and SR-4835 combination therapy elicits 4T1 tumor rejection.

We next assessed if αPD-1 therapy is synergized by CDK12/13 inhibition *in vivo*. To this end, mice were randomized and inoculated with 4T1 tumor cells, and the growth of tumors was assessed every two days (**Figure 4A**). Tumor growth did not decrease significantly in the 4T1 model by SR-4835 treatment alone, although the median survival was indeed extended. Moreover, there was no effect of anti-PD-1 alone on the survival or growth of the tumor. However, SR-4835 and anti-PD-1 combined led to significant regression of tumors, with complete regression in 50% of tumors observed during the time of the study. On day 8, a remarkable difference in tumor size was observed after treatment, and the survival increased significantly in the combination and control treatment groups (**Figure 4B-4E**).

Efficacy of the combination treatment depends on $CD8^+$ T cells.

Next, we explored the role of $CD8^+$ T cells as the crucial T-cell component mediating the synergistic effect of combined SR-4835 and αPD-1 on durable tumor regression. $CD8^+$ T-cell ablation was performed in mice bearing 4T1 tumors by depleting antibodies prior to and when combination treatment was done (**Figure 5A**) and was confirmed by peripheral $CD8^+$ depletion after five days through FACS. No tumor rejection was observed after combination treatment when the cells were depleted of $CD8^+$ T cells (**Figure 5B and 5C**). Ten days post-treatment, the combination group showed an increase in mean tumor volume together with the depletion of CD8 compared with the tumor volume observed in the non-depleted group. CD8 depletion also significantly decreased survival and had few damaging effects compared with the control in terms of survival and the growth of tumors. This result suggests that $CD8^+$ T-cell-mediated immunity at baseline levels serve to limit the growth of 4T1 under basal conditions. Thus, the synergy of SR-4835 with αPD-1 was dependent upon adaptive immunity mediated by $CD8^+$ T cells in this model.

SR-4835 and anti-PD-1 treatment enhance DC activation and intertumoral $CD8^+$ T cells.

To assess the ability of SR-4835 to in inhibit or facilitate an increase in T cell responses mediated by anti-PD-1, we investigated infiltration and activation of T cells in the tumor. To this end, BALB/c mice with established 4T1 tumors were treated as before with SR-4835 and anti-PD-1. Exactly two weeks after treatment initiation, flow cytometry analysis of tumors was performed after harvesting tissues. Compared with the SR-4835 and anti-PD-1 treatments alone, the number of $CD4^+$ and $CD8^+$ T cells that infiltrated the tumors were increased in combination-treated cells (**Figure 6A-6C**). Moreover, the expression of the T cell activation marker was higher in tumor-infiltrating T cells compared with that observed for the controls, with the combination treatment group exhibiting the highest proportion (**Figure 6D and 6E**). To address whether T cell function was enhanced by combination treatment, the dissociated tumors were subjected to intracellular cytokine staining for isolated tumor-infiltrating cells. Compared with the SR-4835 and anti-PD-1 monotherapies, we observed enhanced expression of IFN-γ in $CD8^+$ T cells in the combination

treatment (**Figure 6F**), which also increased the production of granzyme-B (GzB) by $CD8^+$ T cells that infiltrated tumors (**Figure 6G**). Thus, the above data demonstrate that the combination treatment of SR-4835 and anti-PD-1 antibody increased the functionally active T cell numbers in the tumors.

Because SR-4835 induces tumor cell death, we hypothesized that this activity would lead to the activation of local APCs, thereby enhancing antitumor responses. We indeed observed that combination treatment using SR-4835 and anti-PD-1 enhanced the 4T1 tumor-infiltrating $CD11c^+$ DC cell numbers, which also had increased levels of the activation markers CD80, MHC class II (MHCII), and CD86 in comparison to the cells in the monotherapy groups (**Figure 6H-6K**). Therefore, these results suggest that therapy combining SR-4835 and anti-PD-1 increases the activation and function of T cells and APC in the tumor microenvironment compared with the single treatments.

Discussion

A significant milestone in anticancer immunotherapy is the discovery of checkpoint inhibition using monoclonal antibodies targeting CTLA-4 and PD-1/PD-L1(42). Pronounced responses have been observed in clinical trials for several advanced cancers for which there are no alternative treatments (43). It is also apparent that a good efficiency of immunotherapy using single molecules is only observed in a small number of patients, not even for inherently immunogenic tumors (44). Survival was shown to substantially increase when anti-PD-1 was combined with αCTLA-4 blockade, but this treatment also led to a high prevalence of adverse events related to autoimmunity (43). To fully harness the potential of checkpoint immunotherapy, it is important to logically combine and target non-redundant αPD-1/PD-L1 resistance pathways with a concurrent reduction in autoimmunity.

Therapies using small molecules in combination with blockade of the immune checkpoint is an area gathering remarkable interest (45). In pre-clinical studies, the synergistic potential of Bruton's tyrosine kinase inhibitors, αPD-1 blockade combined with indoleamine 2,3-dioxygenase (IDO) inhibitors, and MAP kinase inhibitors, among others, has been observed (46). To the best of our knowledge, this is the first report demonstrating the enhancement of immune-mediated antitumor activity due to pharmacologic inhibition of CDK12/13 in combination with αPD-1 blockade.

Inhibition of CDK12 and 13 disrupts the expression of both kinases and a limited set of genes. These kinases are known to phosphorylate the Ser2 residue of the heptad repeat with RNA Pol II CTD and participate in transcription and co-transcriptional processes (47). According to recent studies, the enhanced transcriptional rate and suppressed cleavage at internal polyadenylation sites is carried out by CDK12, and is also required to facilitate key HR repair protein production (48). In the present study, SR-4835, a CDK12/13 inhibitor that is orally bioavailable and when tested across a panel of 460 kinases, was shown to exhibit outstanding isoform selectivity with only a few off-target interactions (49). SR-4835 exhibits strong anti-TNBC activity in vivo and enhances the anti-cancer activity of olaparib, irinotecan and cisplatin, which are standard TNBC molecules (49).

We observed increased breast tumor cell proliferation and increased *in vitro* cell death due to inhibition of CDK12/13. Apoptotic cell death is not able to stimulate an immune response and is immunologically silent (50). Nevertheless, cell death can be induced using specific chemotherapeutic agents via the ICD mechanism (50). Specific molecules of the DAMP family are released by SR-4835-mediated ICD induction, including HMGB1 release into the extracellular space, cell-surface exposure of calreticulin, and ATP secretion. The innate and adaptive immune responses are activated by the immune system which is in turn alerted by DAMPs(32). The induction of ICD is well reported, and an important role is played by ER stress in bringing about ICD that involves three sensors, ATF6 (activating transcription factor 6), PERK (PKR-like ER-localized eIF2α kinase), which is pathognomonic for ICD, and IRE1 (37). In the present study, we showed that the phosphorylation of IRE1 and eIF2α increased due to SR-4835 treatment. Depletion of ATP may cause ER stress because of the energy requirement for protein assembly, folding, and glycosylation (35). We also observed that CDK12/13 inhibition led to the depletion of intracellular ATP, likely because of a decrease in glycolysis due to decreased glucose uptake. SR-4835 also possesses immunogenic properties.

Our results further show that the CDK12/13 inhibitor SR-4835 is a confirmed agent that induces ICD. We showed that ICD induced by SR-4835 led to enhanced DC activity. We also described a possible mechanism, whereby SR-4835 and anti-PD-1 Ab combination therapy causes an increase in antitumor activity in synergic murine tumor models. An effective immune response was established and subsequent tumor growth stalled upon vaccination with tumor cells killed by SR-4835. SR-4835 enhanced APC and T cell activation within the tumor when combined with anti-PD-1 and improved antitumor efficacy. Additionally, SR-4835 may modulate checkpoint inhibitors and regulatory mechanisms associated with the tumor and immune cell-intrinsic immunosuppression. Specifically, T cells depend on CDK activity, and they are also affected by the antiproliferative activity of SR-4835. Thus, immunostimulatory events associated with ICD may be activated even by a short exposure to SR-4835 without deleteriously affecting the proliferating T cells.

Considering these findings, it will be interesting to assess the promotion of an antitumor immune response via ICD induction mediated by additional CDK inhibitors. Recently, abemaciclib, a CDK4 and CDK6 inhibitor, was shown to enhance antitumor immunity as well as the efficiency of checkpoint blockade, although this occurred through a mechanism different from that used by SR-4835. In tumor cells, abemaciclib appears to induce senescence (and not apoptosis) and initiates a type III IFN response, causing direct MHCI antigen presentation by the tumor cell and repression of PD-1 by CD8 + T cells (51). Therefore, while both abemaciclib and SR-4835 enhance tumor antigenicity, SR-4835 takes a potentially more-controlled and less direct approach via PD-1/PD-L1 axis upregulation and antigen cross-presentation. Thus, it would be worthwhile to determine the interaction of CDK inhibitors of varying selectivity with the immune response.

Intuitively, it makes sense to combine immune checkpoint blockade and ICD-inducing agents, particularly to treat tumors lacking a functional immune response. The antitumor response to radiation therapy that induces ICD is enhanced by checkpoint blockade. Various ongoing clinical trials are evaluating the effect

of combined checkpoint inhibitors with ICD inducers, and these combinations will hopefully benefit an increasing number of patients, broaden the range of the number of treatment indications with existing chemotherapeutics, and reduce their side effects by dose reduction (52, 53). The outcomes of these clinical trials will determine the validity of ICD induction along with immune checkpoint blockade for cancer.

Conclusion

The results of the present study show that an immune-mediated anti-tumor response can be enhanced by pharmacologically targeting CDK12/13 in a combination with checkpoint inhibition using SR-4835. Thus, the results of this study carry significant translational potential, and the combination treatment of SR-4835 with PD-1 blockade should be evaluated in breast cancer treatment.

Abbreviations

ATCC
American Type Culture Collection; ATF6:Activating transcription factor 6; BMDCs:bone marrow-derived DCs; CRT:calreticulin; CTLA4:cytotoxic T-lymphocyte associated protein 4; DAMPs; damage-associated molecular patterns; DC:dendritic cells; Dox:doxorubicin; DMSO:dimethyl sulfoxide; ER:endoplasmic reticulum; EGFR2:human epidermal growth factor receptor 2; FBS:fetal bovine serum; GzB:granzyme-B; HMGB1:high mobility group box 1; ICD:immunogenic cell death; IDO:Indoleamine 2,3-dioxygenase; IRE1:inositol-requiring enzyme 1; MHCII:MHC class II; PD-1:programmed death 1; PERK:PKR-like ER-localized eIF2α kinase; PR:progesterone receptor; PRM:proline-rich motif; TILs:tumor-infiltrating lymphocytes; TNBC:triple-negative breast cancer; UPR:unfolded protein response.

Declarations

Acknowledgements

This work was supported by Sichuan Provincial Commission of Health and Family Planning (Grant NO. 17PJ099).

Authors' contributions

YL, CW and LT developed the hypothesis, designed the experiments, and revised the manuscript. YL, HZ, QL, PZ and XH performed the experiments and statistical analyses.

Availability of data and materials

All data generated or analyzed during this study are included in this published article.

Ethics approval and consent to participate

This study was approved by the Ethical Committee of Sichuan Academy of Medical Sciences & Sichuan Provincial People's Hospital.

Consent for publication

Informed consent was obtained from all individual participants included in the study.

Competing interests

The authors declare that they have no conflicts of interest.

References

1. Waks AG & Winer EP (2019) Breast Cancer Treatment: A Review. *JAMA* 321(3):288-300.
2. Giuliano M*, et al.* (2019) Endocrine treatment versus chemotherapy in postmenopausal women with hormone receptor-positive, HER2-negative, metastatic breast cancer: a systematic review and network meta-analysis. *Lancet Oncol* 20(10):1360-1369.
3. Goutsouliak K*, et al.* (2019) Towards personalized treatment for early stage HER2-positive breast cancer. *Nat Rev Clin Oncol*.
4. Marra A, Viale G, & Curigliano G (2019) Recent advances in triple negative breast cancer: the immunotherapy era. *BMC Med* 17(1):90.
5. El Hachem G, Gombos A, & Awada A (2019) Recent advances in understanding breast cancer and emerging therapies with a focus on luminal and triple-negative breast cancer. *F1000Res* 8.
6. Bergin ART & Loi S (2019) Triple-negative breast cancer: recent treatment advances. *F1000Res* 8.
7. Wilkinson RW & Leishman AJ (2018) Further Advances in Cancer Immunotherapy: Going Beyond Checkpoint Blockade. *Front Immunol* 9:1082.
8. Zhang H & Chen J (2018) Current status and future directions of cancer immunotherapy. *J Cancer* 9(10):1773-1781.
9. Zhou X, Liu R, Qin S, Yu R, & Fu Y (2016) Current Status and Future Directions of Nanoparticulate Strategy for Cancer Immunotherapy. *Curr Drug Metab* 17(8):755-762.
10. Basu A*, et al.* (2019) Immunotherapy in breast cancer: Current status and future directions. *Adv Cancer Res* 143:295-349.
11. Dobosz P & Dzieciatkowski T (2019) The Intriguing History of Cancer Immunotherapy. *Front Immunol* 10:2965.
12. Wu X*, et al.* (2019) Application of PD-1 Blockade in Cancer Immunotherapy. *Comput Struct Biotechnol J* 17:661-674.
13. Silva MA*, et al.* (2020) Biomarker recommendation for PD-1/PD-L1 immunotherapy development in pediatric cancer based on digital image analysis of PD-L1 and immune cells. *J Pathol Clin Res*.

14. Bellmunt J, Powles T, & Vogelzang NJ (2017) A review on the evolution of PD-1/PD-L1 immunotherapy for bladder cancer: The future is now. *Cancer Treat Rev* 54:58-67.
15. Ni L & Lu J (2018) Interferon gamma in cancer immunotherapy. *Cancer Med* 7(9):4509-4516.
16. Wang S, He Z, Wang X, Li H, & Liu XS (2019) Antigen presentation and tumor immunogenicity in cancer immunotherapy response prediction. *Elife* 8.
17. Perduca V*, et al.* (2019) Stem cell replication, somatic mutations and role of randomness in the development of cancer. *Eur J Epidemiol* 34(5):439-445.
18. Savola P*, et al.* (2017) Somatic mutations in clonally expanded cytotoxic T lymphocytes in patients with newly diagnosed rheumatoid arthritis. *Nat Commun* 8:15869.
19. Galluzzi L, Buque A, Kepp O, Zitvogel L, & Kroemer G (2017) Immunogenic cell death in cancer and infectious disease. *Nat Rev Immunol* 17(2):97-111.
20. Huang FY*, et al.* (2018) Induction of enhanced immunogenic cell death through ultrasound-controlled release of doxorubicin by liposome-microbubble complexes. *Oncoimmunology* 7(7):e1446720.
21. Serrano-Del Valle A, Anel A, Naval J, & Marzo I (2019) Immunogenic Cell Death and Immunotherapy of Multiple Myeloma. *Front Cell Dev Biol* 7:50.
22. Krajewska M*, et al.* (2019) CDK12 loss in cancer cells affects DNA damage response genes through premature cleavage and polyadenylation. *Nat Commun* 10(1):1757.
23. Quereda V*, et al.* (2019) Therapeutic Targeting of CDK12/CDK13 in Triple-Negative Breast Cancer. *Cancer Cell* 36(5):545-558 e547.
24. Lui GYL, Grandori C, & Kemp CJ (2018) CDK12: an emerging therapeutic target for cancer. *J Clin Pathol* 71(11):957-962.
25. Zhang J*, et al.* (2018) Cyclin D-CDK4 kinase destabilizes PD-L1 via cullin 3-SPOP to control cancer immune surveillance. *Nature* 553(7686):91-95.
26. Deng J*, et al.* (2018) CDK4/6 Inhibition Augments Antitumor Immunity by Enhancing T-cell Activation. *Cancer Discov* 8(2):216-233.
27. Hossain DMS*, et al.* (2018) Dinaciclib induces immunogenic cell death and enhances anti-PD1-mediated tumor suppression. *J Clin Invest* 128(2):644-654.
28. Tong J*, et al.* (2018) Mcl-1 Phosphorylation without Degradation Mediates Sensitivity to HDAC Inhibitors by Liberating BH3-Only Proteins. *Cancer Res* 78(16):4704-4715.
29. Tong J*, et al.* (2017) Mcl-1 Degradation Is Required for Targeted Therapeutics to Eradicate Colon Cancer Cells. *Cancer Res* 77(9):2512-2521.
30. Tong J, Tan S, Zou F, Yu J, & Zhang L (2017) FBW7 mutations mediate resistance of colorectal cancer to targeted therapies by blocking Mcl-1 degradation. *Oncogene* 36(6):787-796.
31. Kroemer G, Galluzzi L, Kepp O, & Zitvogel L (2013) Immunogenic cell death in cancer therapy. *Annu Rev Immunol* 31:51-72.
32. Fahmueller YN*, et al.* (2013) Immunogenic cell death biomarkers HMGB1, RAGE, and DNAse indicate response to radioembolization therapy and prognosis in colorectal cancer patients. *Int J Cancer*

132(10):2349-2358.

33. Zhou J*, et al.* (2019) Immunogenic cell death in cancer therapy: Present and emerging inducers. *J Cell Mol Med* 23(8):4854-4865.
34. Wang YJ, Fletcher R, Yu J, & Zhang L (2018) Immunogenic effects of chemotherapy-induced tumor cell death. *Genes Dis* 5(3):194-203.
35. Martins I*, et al.* (2014) Molecular mechanisms of ATP secretion during immunogenic cell death. *Cell Death Differ* 21(1):79-91.
36. van Vloten JP, Workenhe ST, Wootton SK, Mossman KL, & Bridle BW (2018) Critical Interactions between Immunogenic Cancer Cell Death, Oncolytic Viruses, and the Immune System Define the Rational Design of Combination Immunotherapies. *J Immunol* 200(2):450-458.
37. Radogna F & Diederich M (2018) Stress-induced cellular responses in immunogenic cell death: Implications for cancer immunotherapy. *Biochem Pharmacol* 153:12-23.
38. Kepp O*, et al.* (2015) eIF2alpha phosphorylation as a biomarker of immunogenic cell death. *Semin Cancer Biol* 33:86-92.
39. Teske BF*, et al.* (2011) The eIF2 kinase PERK and the integrated stress response facilitate activation of ATF6 during endoplasmic reticulum stress. *Mol Biol Cell* 22(22):4390-4405.
40. van der Harg JM*, et al.* (2017) The UPR reduces glucose metabolism via IRE1 signaling. *Biochim Biophys Acta Mol Cell Res* 1864(4):655-665.
41. Garg AD*, et al.* (2015) Molecular and Translational Classifications of DAMPs in Immunogenic Cell Death. *Front Immunol* 6:588.
42. Buchbinder EI & Desai A (2016) CTLA-4 and PD-1 Pathways: Similarities, Differences, and Implications of Their Inhibition. *Am J Clin Oncol* 39(1):98-106.
43. Puri S & Shafique M (2020) Combination checkpoint inhibitors for treatment of non-small-cell lung cancer: an update on dual anti-CTLA-4 and anti-PD-1/PD-L1 therapies. *Drugs Context* 9.
44. Seidel JA, Otsuka A, & Kabashima K (2018) Anti-PD-1 and Anti-CTLA-4 Therapies in Cancer: Mechanisms of Action, Efficacy, and Limitations. *Front Oncol* 8:86.
45. Hayashi H & Nakagawa K (2019) Combination therapy with PD-1 or PD-L1 inhibitors for cancer. *Int J Clin Oncol*.
46. Deken MA*, et al.* (2016) Targeting the MAPK and PI3K pathways in combination with PD1 blockade in melanoma. *Oncoimmunology* 5(12):e1238557.
47. Greenleaf AL (2019) Human CDK12 and CDK13, multi-tasking CTD kinases for the new millenium. *Transcription* 10(2):91-110.
48. Liang K*, et al.* (2015) Characterization of human cyclin-dependent kinase 12 (CDK12) and CDK13 complexes in C-terminal domain phosphorylation, gene transcription, and RNA processing. *Mol Cell Biol* 35(6):928-938.
49. Anonymous (2019) CDK12/13 Inhibitor SR-4835 Is Active in Triple-Negative Breast Cancer. *Cancer Discov* 9(12):1644.

50. Zhu J*, et al.* (2017) Resistance to cancer immunotherapy mediated by apoptosis of tumor-infiltrating lymphocytes. *Nat Commun* 8(1):1404.
51. Tamura K (2019) Differences of cyclin-dependent kinase 4/6 inhibitor, palbociclib and abemaciclib, in breast cancer. *Jpn J Clin Oncol* 49(11):993-998.
52. Kepp O, Zitvogel L, & Kroemer G (2019) Clinical evidence that immunogenic cell death sensitizes to PD-1/PD-L1 blockade. *Oncoimmunology* 8(10):e1637188.
53. Hodge JW*, et al.* (2013) Chemotherapy-induced immunogenic modulation of tumor cells enhances killing by cytotoxic T lymphocytes and is distinct from immunogenic cell death. *Int J Cancer* 133(3):624-636.

Figures

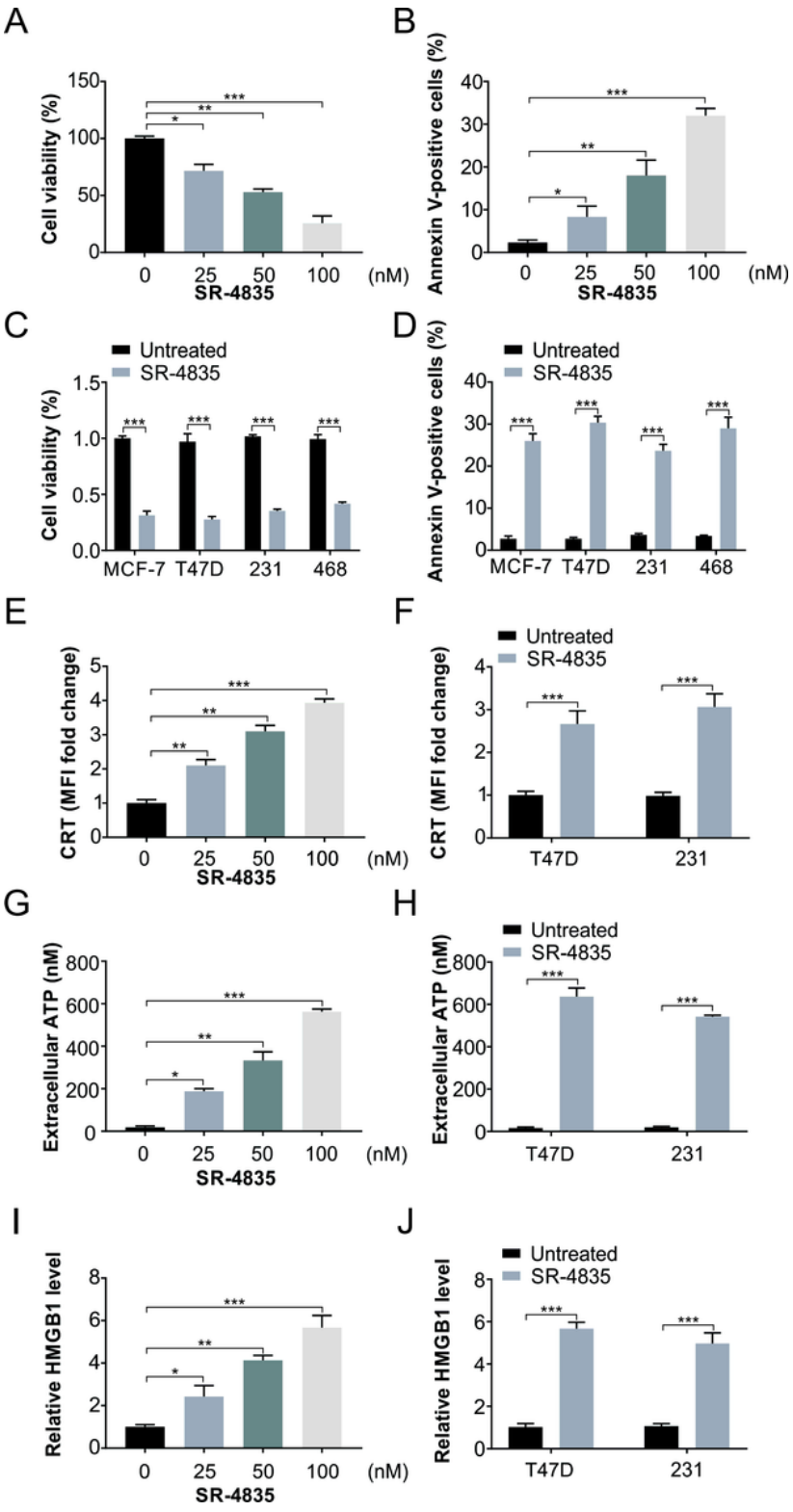

Figure 1

SR-4835 induces cell death, CRT translocation, ATP secretion and HMGB1 release in breast cancer cells. (A) Cell viability was analyzed in 4T1 cells treated with SR-4835 at indicated concentration for 48 hours. (B) Apoptosis was analyzed by flow cytometry in 4T1 cells treated with SR-4835 at indicated concentration for 24 hours. (C) Cell viability was analyzed in indicated cells treated with 100nM SR-4835 for 48 hours. (D) Apoptosis was analyzed by flow cytometry in indicated cells treated with 100nM SR-

4835 for 24 hours. (E) CRT translocation was detected by flow cytometry in 4T1 cells treated with SR-4835 at indicated concentration for 24 hours. (F) CRT translocation was detected by flow cytometry in indicated cells treated with 100nM SR-4835 for 24 hours. (G) ATP content was detected in the media of 4T1 cells treated with SR-4835 at indicated concentration for 24 hours by a chemiluminescent kit. (H) ATP content was detected in the media of indicated cells treated with 100nM SR-4835 for 24 hours by a chemiluminescent kit. (I) HMGB1 content was detected in the media of 4T1 cells treated with SR-4835 at indicated concentration for 24 hours. (H) ATP content was detected in the media of indicated cells treated with 100nM SR-4835 for 24 hours. The results were expressed as the means ± SD of three independent experiments. *, P<0.05; **, P<0.01; ***, P<0.001.

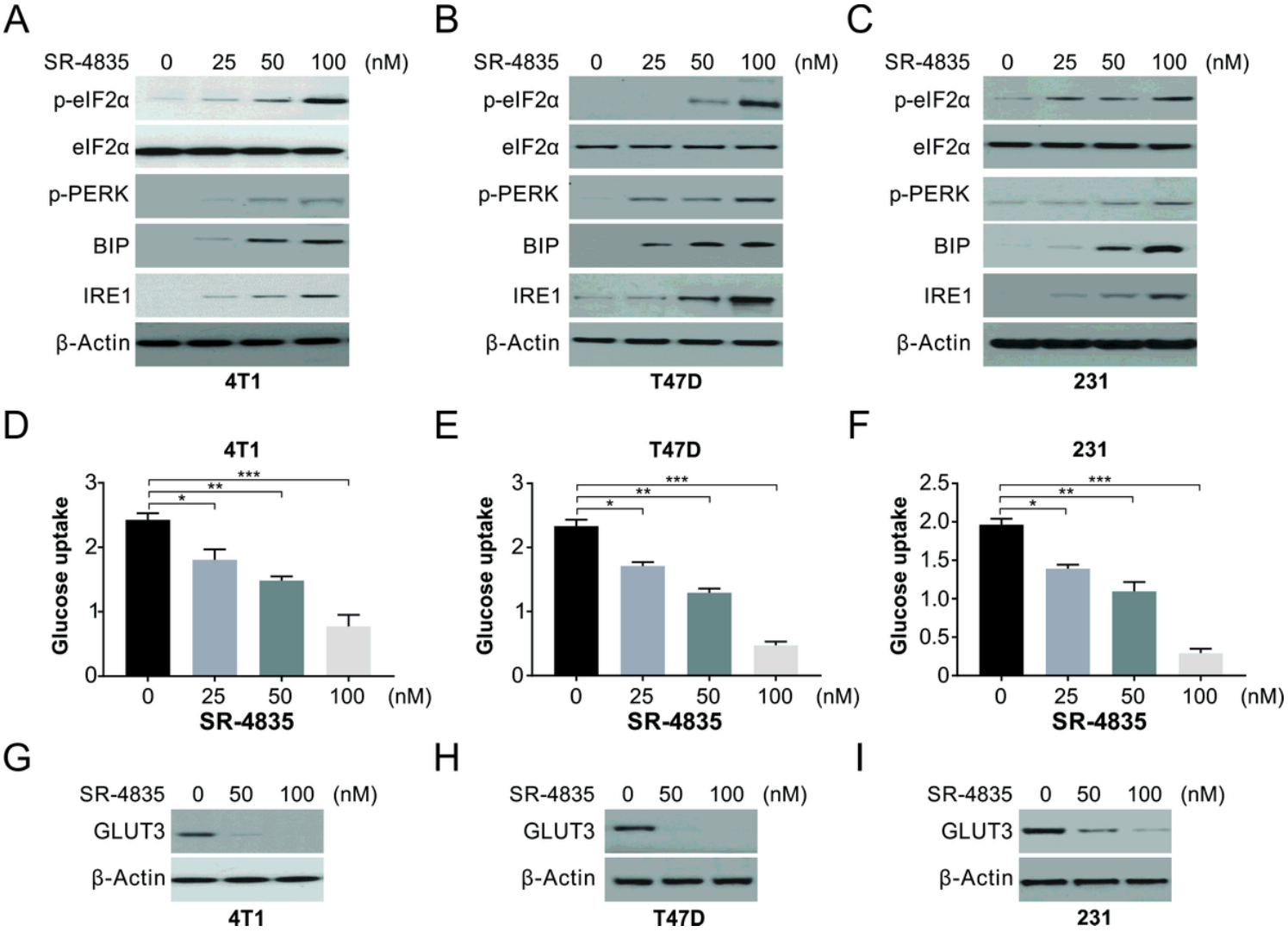

Figure 2

SR-4835 induces ER stress in breast cancer cells. (A) Western blotting of indicated protein in 4T1 cells treated with SR-4835 at indicated concentration for 24 hours. (B) Western blotting of indicated protein in T47D cells treated with SR-4835 at indicated concentration for 24 hours. (C) Western blotting of indicated protein in MDA-MB-231 cells treated with SR-4835 at indicated concentration for 24 hours. (D) Glucose uptake of indicated protein in 4T1 cells treated with SR-4835 at indicated concentration for 24 hours. (E) Glucose uptake of indicated protein in T47D cells treated with SR-4835 at indicated concentration for 24

hours. (F) Glucose uptake of indicated protein in MDA-MB-231 cells treated with SR-4835 at indicated concentration for 24 hours. (G) Western blotting of GLUT3 in 4T1 cells treated with SR-4835 at indicated concentration for 24 hours. (H) Western blotting of GLUT3 in T47D cells treated with SR-4835 at indicated concentration for 24 hours. (I) Western blotting of GLUT3 in MDA-MB-231 cells treated with SR-4835 at indicated concentration for 24 hours. The results were expressed as the means ± SD of three independent experiments. *, P<0.05; **, P<0.01; ***, P<0.001.

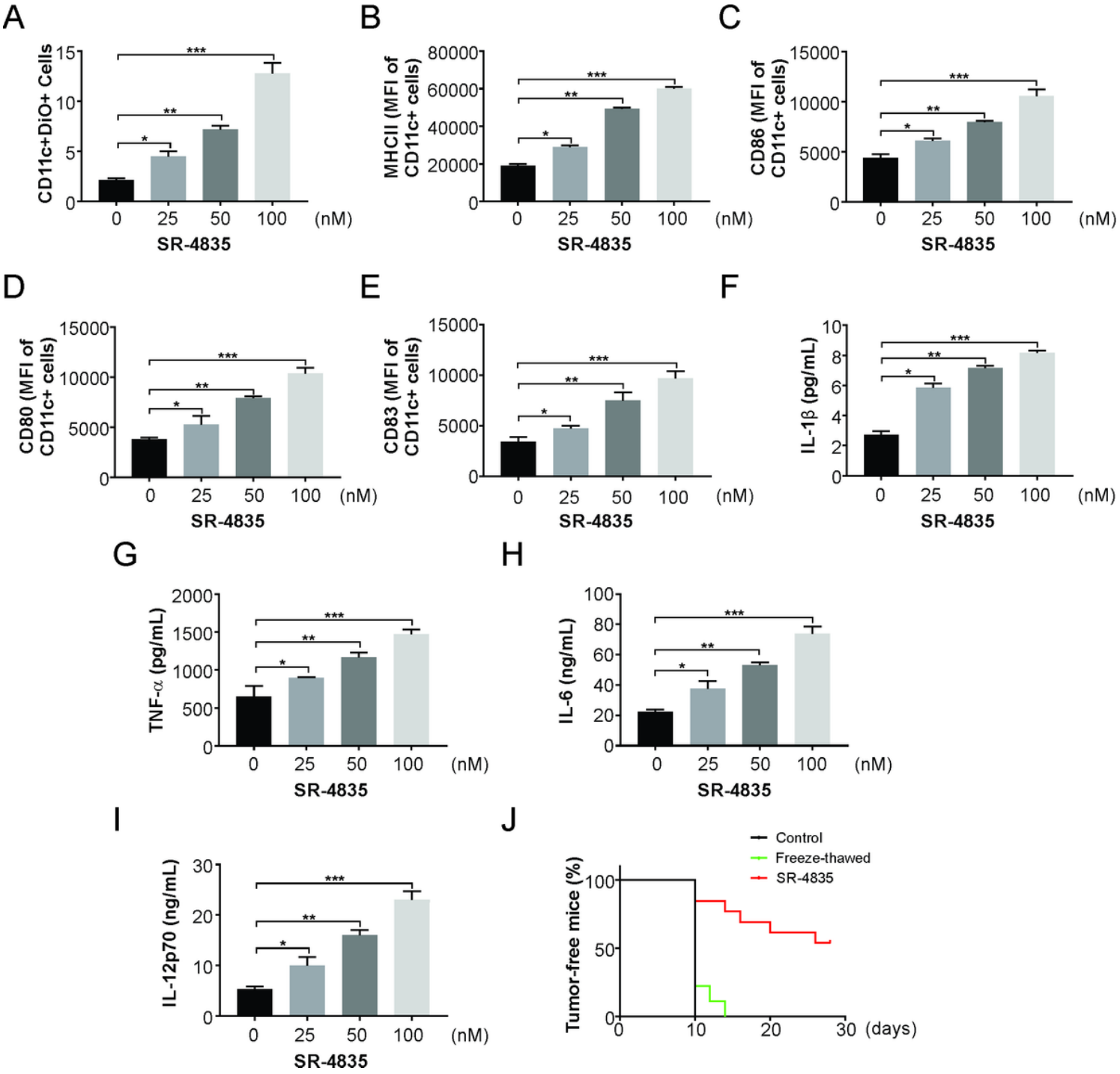

Figure 3

SR-4835 promotes DC cells activation. DiO-labeled 4T1 cells were treated with the indicated concentrations of SR-4835 for 24 hours and then cocultured with BMDCs for an additional 24 hours. (A)

The percentage of CD11c+ DCs with engulfed tumor cells was assessed by flow cytometry. (B) MHCII, (C) CD86, (D) CD80, (E) CD83 of CD11c+DC cells after coculture were analyzed by flow cytometry. Secretion of (F) IL-1β, (G) TNF-α, (H) IL-6, (I) IL-12p70 into the coculture supernatant was determined by MSD assay. (J) 4T1 cells either treated in vitro with SR-4835 or freeze-thawed were inoculated s.c. into mice. After 10 days, mice were rechallenged with live 4T1 cells. Shown is the percentage of tumor-free mice pooled from 2 independent experiments. The results were expressed as the means ± SD of three independent experiments. *, P<0.05; **, P<0.01; ***, P<0.001.

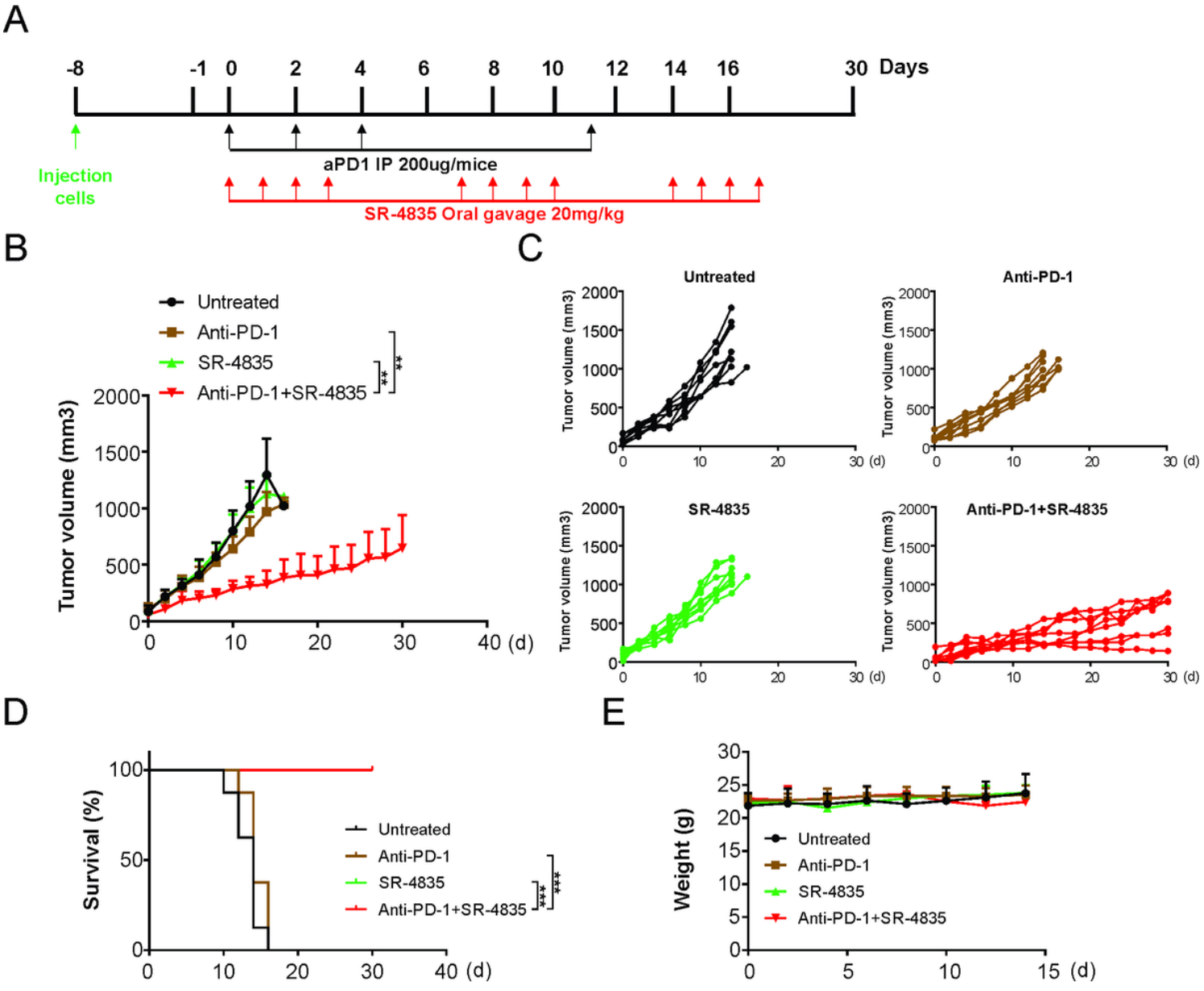

Figure 4

SR-4835 enhances PD-1 blockade activities in syngeneic mouse model. BALB/c mice were inoculated with 5×105 4T1 cells subcutaneously in the right thoracic flank. When tumors reached between 50 and 100mm3, mice were then randomized to four treatment groups and treated with SR-4835 (20mg/kg), anti-PD1 antibody (200μg/mice), or their combination. (n=8). (A) A schematic view of the treatment plan. (B) Tumor growth curves measured every 2 days. (C) Individual tumor volume over time. (D) Kaplan-Meier

survival curves for each group. (E) Plots of mice weight measured every 2 days. Data represent at least 2 independent experiments. ***, P < 0.001; **, P < 0.01.

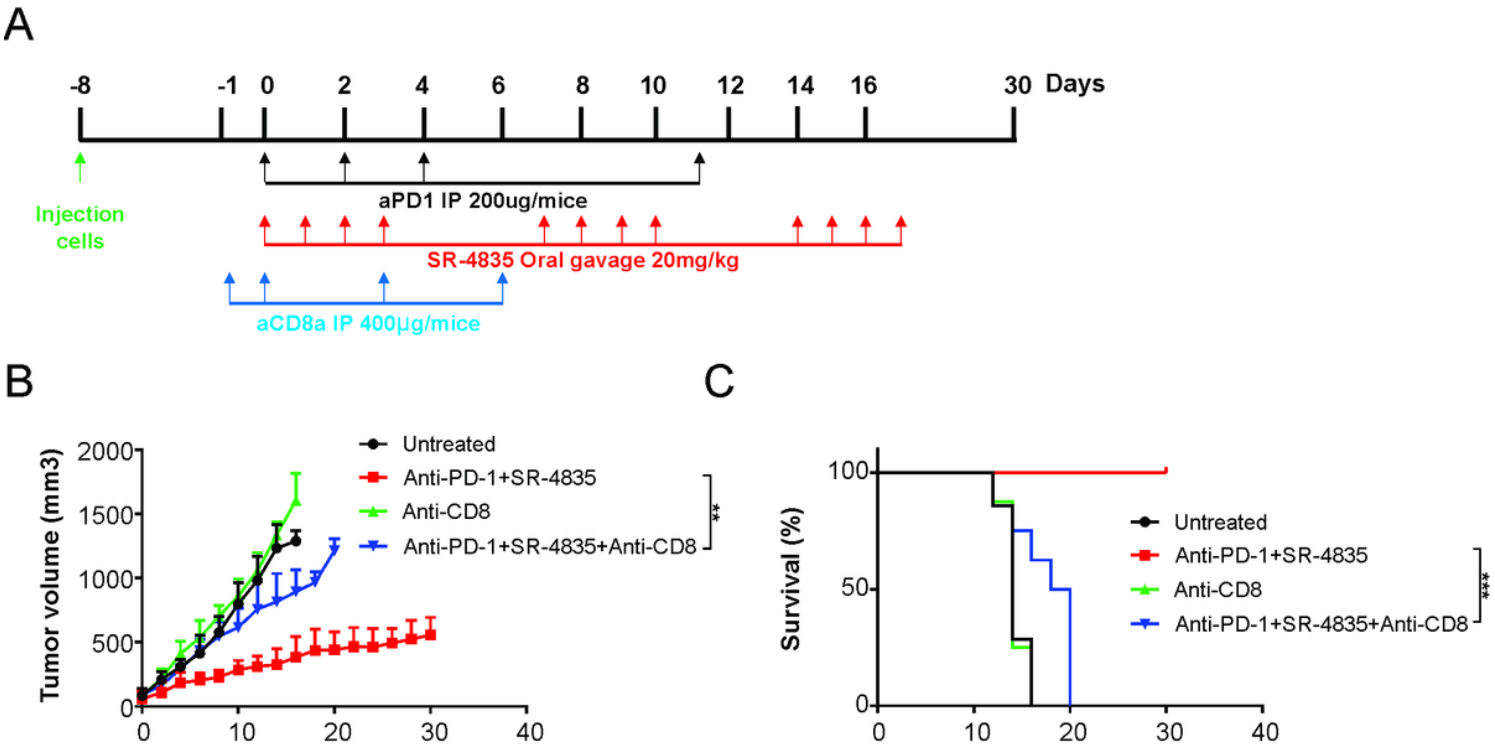

Figure 5

SR-4835 and PD-1 blockade induced tumor suppression in a CD8+ T cell-dependent manner. BALB/c mice were inoculated with 5×105 4T1 cells subcutaneously in the right thoracic flank. When tumors reached between 50 and 100mm3, mice were then randomized to four treatment groups and treated with anti-CD8 antibody and the combination of SR-4835 and anti-PD1 antibody. (n=8). (A) A schematic view of the treatment plan. (B) Tumor growth curve measured every 2 days. (C) Kaplan-Meier survival curves for each group. Data represent at least 2 independent experiments. ***, P < 0.001; **, P < 0.01.

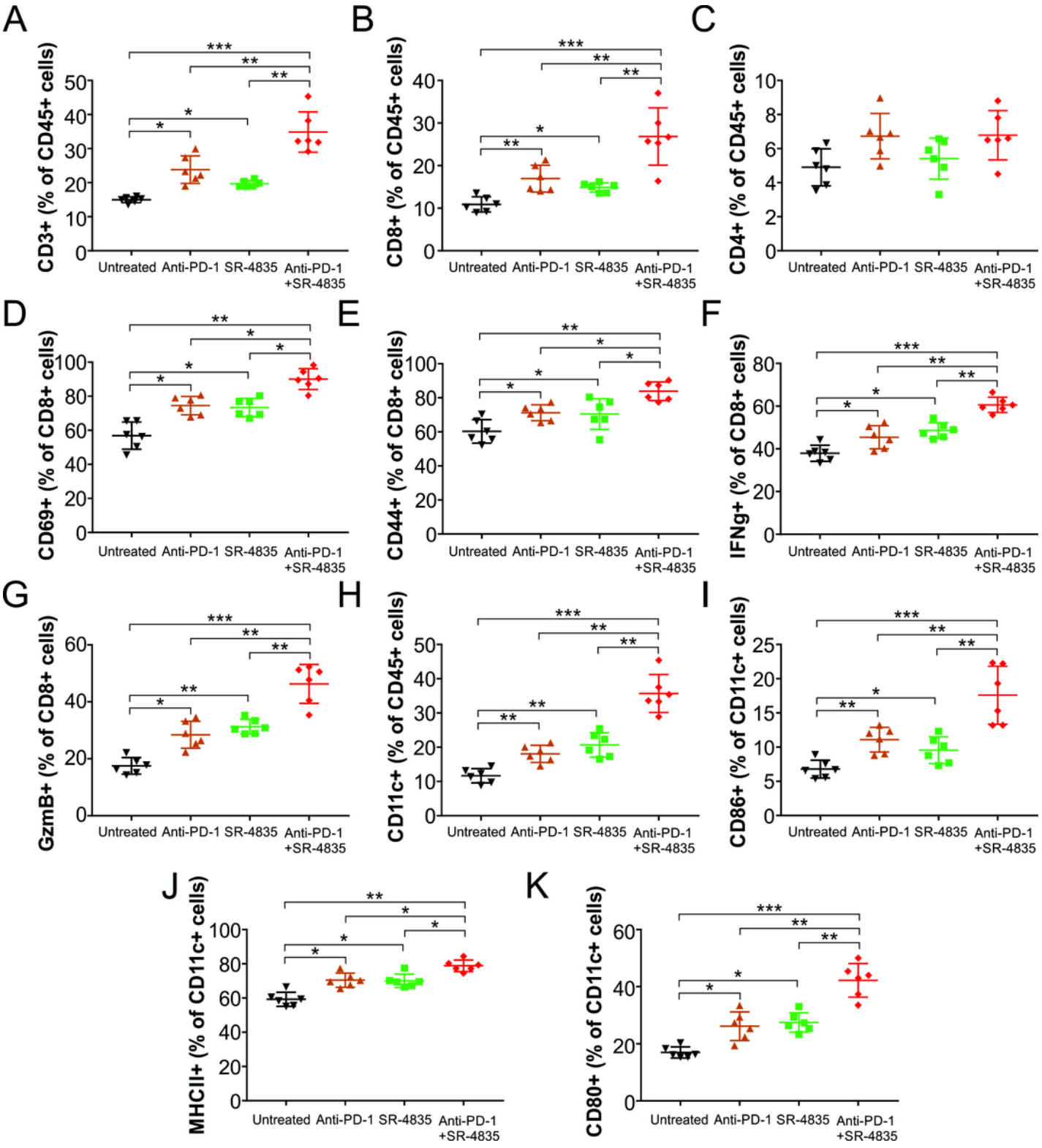

Figure 6

SR-4835 and PD-1 blockade induces immune cell infiltration and activation in tumors. Mice with established 4T1 tumors were treated with SR-4835 and anti-PD-1 Ab as in Figure 4. Tumors were isolated on day 10, and immune cells were analyzed by flow cytometry (n=6 mice/group). Shown are the population of tumor-infiltrating (A) CD3+ T cells in CD45+ cells, (B) CD8+ T cells in CD45+ cells, (C) CD4+ T cells in CD45+ cells. (D) CD69+ T cells in CD8+ cells, (E) CD44+ T cells in CD8+ cells. For the detection

of intracellular cytokines, harvested TILs were stimulated with PMA and ionomycin in the presence of brefeldin A for 4 hours. Shown are the population of (F) IFN-γ+ and (G) GzmB+ in CD8+ T cells. For the detection of DC cells activation. Shown are the population of (H) CD11c+ cells in CD45+ cells, (I) CD86+, (J) MHCII+, and (K) CD80+ cells in CD11c+ cells. The results were expressed as the means ± SD of three independent experiments. *, $P<0.05$; **, $P<0.01$; ***, $P<0.001$.